

Modeling groundwater and heat flow subject to freezing and thawing

Volker Clausnitzer¹, Vladimir Mirnyy²

¹DHI-WASY GmbH, Volmerstr. 8, 12489 Berlin, Germany, vcl@dhigroup.com

²Lindenstr. 30A, 12555 Berlin, Germany, vladimir@mirnyy.eu

Abstract

A newly developed FEFLOW plug-in module, piFreeze, provides simulation capabilities to cover freezing and thawing of subsurface water. The governing balance equations account for the respective volume fractions of frozen and liquid water and for the density difference between both phases. Extensions have been developed for both unsaturated and saturated conditions. Constitutive relations describe the temperature dependency of the heat capacity including the latent heat associated with the phase change, of permeability and fluid viscosity, and of the thermal conductivity. A flexible empirical expression describes the local freezing progress in terms of liquid/ice mass fractioning over a finite temperature range around the freezing point.

Application potential for FEFLOW with piFreeze is seen wherever natural or artificially induced freezing and thawing processes significantly affect the groundwater flow, for example in mining, construction, permafrost conditions, and geothermal energy.

Key words: Numerical modeling, FEFLOW, piFreeze, groundwater, freezing, thawing, permafrost, artificial ground freezing

Notation

Subscripts a, l, s, i identify air, liquid, solid (other than ice), and ice phases, respectively.

ε_x	Volume fraction of phase x
ε	Flow-accessible volume fraction ('porosity'), $\varepsilon = \varepsilon_a + \varepsilon_l$
ρ_x	Density of phase x
φ	Mass fraction of liquid water to total (liquid + frozen) water, $\varphi = \frac{\varepsilon_l \rho_l}{\varepsilon_l \rho_l + \varepsilon_i \rho_i}$
T	Temperature
L_f	Latent heat of freezing/melting
λ	Effective thermal conductivity
λ_x	Thermal conductivity of phase x
C	Effective volumetric heat capacity
C_x	Volumetric heat capacity of phase x
s	Liquid-phase saturation, $s = \varepsilon_l / \varepsilon$
h	Liquid-phase pressure head
Q	Liquid-phase volumetric source
Q_f	Liquid-phase volumetric source from freezing/melting
S_o	Liquid-phase specific storage coefficient
K_s	Saturated hydraulic conductivity
$K_{r,s}(s)$	Hydraulic-conductivity reduction factor due to saturation (empirical relation)
$K_{r,f}(\varphi)$	Hydraulic-conductivity reduction factor due to melting/freezing (empirical relation)
K	Effective unsaturated hydraulic conductivity, $K = K_s K_{r,s}(s) K_{r,f}(\varphi)$
q	Liquid-phase (Darcy) flux, $q = -K \nabla(h + z)$

Theory

We assume that the respective volume fractions of air, liquid, solid, and ice add up to unity everywhere and at all times,

$$1 = \varepsilon_a + \varepsilon_l + \varepsilon_s + \varepsilon_i$$

The local transition from ice to liquid and vice versa is described by the ‘freezing function’ $\varphi(T)$, shown in Fig. 1 as both an empirical linear and a smooth higher-order relation.

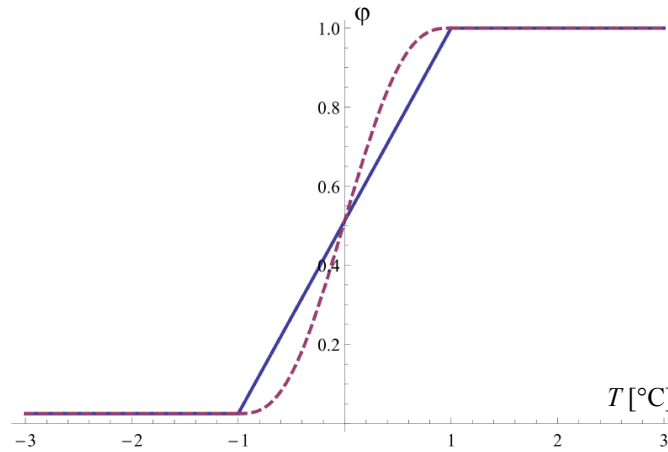


Figure 1 Alternative empirical shapes expressing the local mass fraction of liquid water to total (liquid + frozen) water as a function of temperature.

Under partially saturated conditions ($\varepsilon_a > 0, s < 1$), it is assumed that water as it transitions from liquid to ice phase expands into space occupied by the air phase. As no water is transferred across the boundary of a representative elementary volume (REV) due to freezing/melting, the local water mass remains constant (i.e., $\varepsilon_l \rho_l + \varepsilon_i \rho_i = \text{const.}$ with respect to φ) so that

$$\varepsilon_l = \varphi \left(\varepsilon_l + \varepsilon_i \frac{\rho_i}{\rho_l} \right) \quad \text{and} \quad \varepsilon_i = (1 - \varphi) \left(\varepsilon_l \frac{\rho_l}{\rho_i} + \varepsilon_i \right)$$

In contrast, under fully saturated conditions ($\varepsilon_a = 0, s = 1$), there is no air present and water must transfer across the REV boundary due to the change in density as it transitions from liquid to ice phase or vice versa. In this case there is a fixed total local volume fraction available to water, (i.e., $\varepsilon_l + \varepsilon_i = 1 - \varepsilon_s = \text{const.}$ with respect to φ), and it follows that

$$\varepsilon_l = \frac{\varphi (\varepsilon_l + \varepsilon_i) \frac{\rho_i}{\rho_l}}{1 - \varphi \left(1 - \frac{\rho_i}{\rho_l} \right)} \quad \text{and} \quad \varepsilon_i = \frac{(1 - \varphi) (\varepsilon_l + \varepsilon_i)}{1 - \varphi \left(1 - \frac{\rho_i}{\rho_l} \right)}$$

Mass-conservation considerations give rise to an additional source term Q_f appearing in the Richards equation

$$S_o s \frac{\partial h}{\partial t} + \varepsilon \frac{\partial h}{\partial t} \frac{\partial h}{\partial t} + \nabla \cdot \mathbf{q} = Q + Q_f$$

with

$$Q_f = 0 \quad \text{for} \quad s < 1$$

and

$$Q_f = -\frac{\partial \varphi}{\partial T} \frac{\partial T}{\partial t} \left(\rho_i \frac{\partial \varepsilon_i}{\partial \varphi} + \frac{\partial \varepsilon_i}{\partial \varphi} \right) \text{ for } s = 1$$

An effective thermal conductivity is presumed to follow from the local phase composition, considering the contribution from the air phase as negligible,

$$\lambda = \varepsilon_l \lambda_l + \varepsilon_s \lambda_s + \varepsilon_i \lambda_i$$

A similar assumption is made for the heat capacity which must further account for the latent heat of freezing/melting associated with any change in the local ice fraction,

$$C = \varepsilon_l C_l + \varepsilon_s C_s + \varepsilon_i C_i - L_f \rho_i \frac{\partial \varepsilon_i}{\partial \varphi} \frac{\partial \varphi}{\partial T}$$

As shown in Figure 2, general agreement was observed between predictions for the “Frozen Wall” Benchmark (McKenzie et al. 2007) by FEFLOW (Diersch 2014) with piFreeze and by SUTRA-ICE, which handles fully saturated conditions (McKenzie et al. 2007).

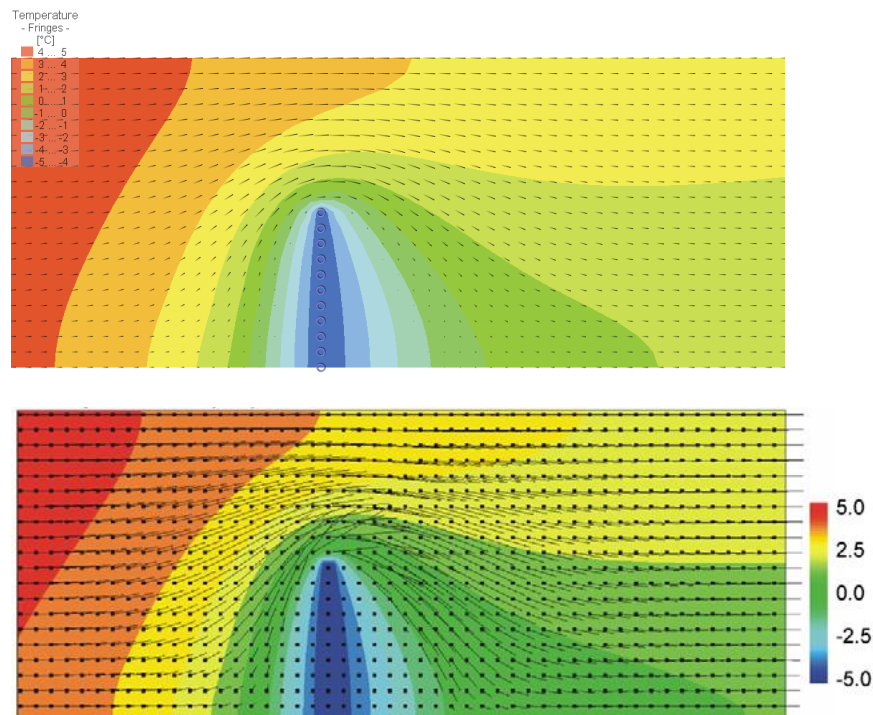


Figure 2 “Frozen Wall” Benchmark, Temperature distribution and flow field after 800 d computed by FEFLOW with piFreeze (top) and SUTRA-ICE (bottom).

Application

A hypothetical three-dimensional freeze-wall investigation is illustrated in Figure 3. Below, Figure 4 clearly shows the effect of the prevailing hydraulic-head gradient on the freeze-wall closure dynamics, the flow field, and the temperature distribution.

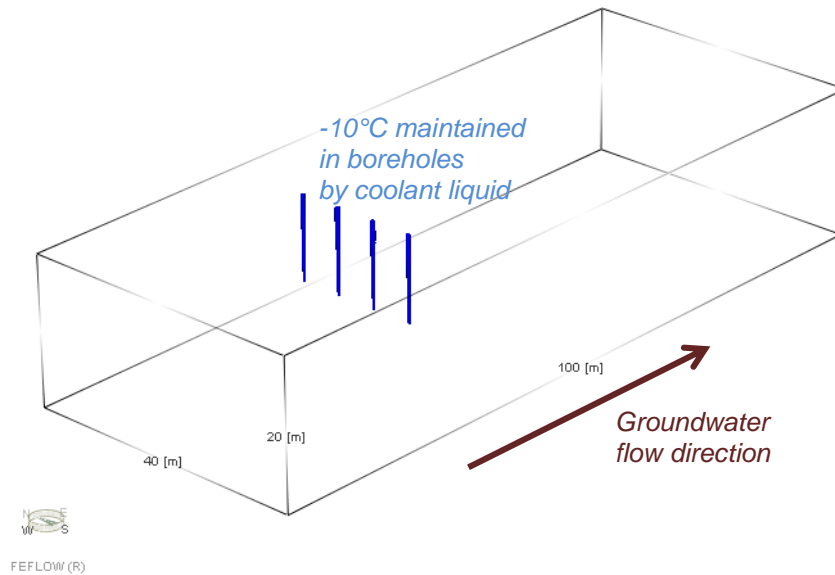


Figure 3 3D Freeze-wall study.

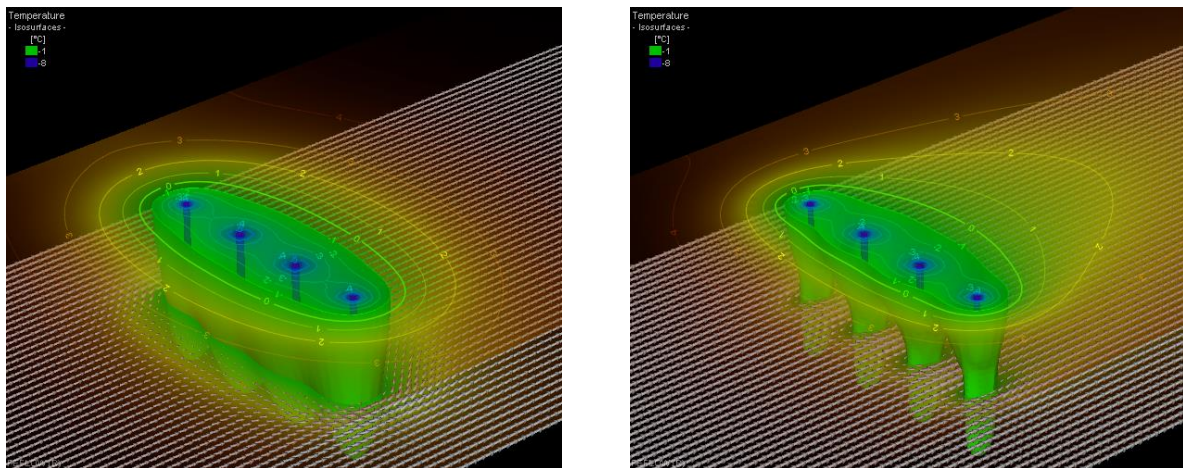


Figure 4 Temperature distribution two years after initiation of freezing compared for a groundwater hydraulic-head gradient of 10^{-4} (left) and 10^{-3} (right).

References

- Diersch, H.-J. G (2014) FEFLOW: Finite Element Modeling of Flow, Mass and Heat Transport in Porous and Fractured Media, Springer, Berlin.
- J. M. McKenzie, C. I. Voss, and D. I. Siegel (2007) Groundwater flow with energy transport and water-ice phase change: Numerical simulations, benchmarks, and application to freezing in peat bogs. *Advances in Water Resources*, 30(4):966–983.